CONCEPTUAL DESIGN OF AN "UMBRELLA" SPACECRAFT FOR ORBITAL DEBRIS SHIELDING

Daniel M. Thomson[(1)], Aleksandr Cherniaev[(2)], Igor Telichev[(2)]

[(1)] ETSEIB, Universitat Politècnica de Catalunya (Barcelona Tech.), Av. Diagonal 647, Barcelona, Spain, 08028, E-mail: daniel.thomson@estudiant.upc.edu

[(2)] University of Manitoba, Department of Mechanical Engineering, E2-327 EITC, 75A Chancellors Circle 2500 Winnipeg, Manitoba, Canada R3T 5V6, E-mail: aleksandr.cherniaev@umanitoba.ca, igor.telichev@umanitoba.ca
Phone: (204) 474-9812, Fax: (204) 275-7507

ABSTRACT

Current protection techniques leave spacecraft vulnerable to objects between approximately 1 and 10 cm. This paper summarizes the conceptual design of a space vehicle capable of shielding spacecraft from objects in this range of sizes, which was made to study the feasibility of such a method for spacecraft protection. The design was divided into three stages: first, using SPH simulations, a multi-layer shield capable of defeating large projectiles was designed; next, a deployment mechanism that allowed the shield to be stored compactly for launch was designed and analyzed using a vector-based kinematics and dynamics method; finally, a general design of the service module was made. The final design has feasible dimensions for a spacecraft to be placed in Low Earth Orbit (LEO) and consists of an eight-layer shield with an umbrella-inspired deployment mechanism.

KEYWORDS: ORBITAL DEBRIS, SPACECRAFT SHIELDING, HYPERVELOCITY IMPACT

1. INTRODUCTION

The threat posed by orbital debris (OD) has been a growing concern for many years; ever since the hazard was first acknowledged in the early 1980's it has been the subject of numerous studies, and it continuously increases the demands on spacecraft protection systems, thus leading to an increase in the weight, size and cost of spacecraft [1].

In addition, current protection techniques are not capable of protecting spacecraft from the whole range of orbital debris; there is a group of objects, from approximately 1 to 10 cm in diameter to which even well protected spacecraft remain vulnerable [2]. Therefore, the objective of this project was the design of a conceptual space vehicle to act as a shield to protect other larger and higher-value spacecraft from orbital debris, and to explore the feasibility of such a measure for orbital debris protection.

Larger and higher-value spacecraft, such as manned space stations or refueling/docking stations, will likely become more common in the future, and due to their larger size and long expected lifetimes, they will be more susceptible to unforeseeable impacts from debris. Therefore, the objective for this project, motivated by the ideas circulated in the early era of space debris research in 90's, was the design of a conceptual space vehicle to act as a relatively inexpensive, external form of passive protection from orbital debris for other larger and higher-value spacecraft [3-7].

The proposed "defender" vehicle would consist of a shield capable of protecting these spacecraft from the larger objects in the 1-10 cm range. A deployment mechanism would allow the shield to be stored compactly during launch and deployed once in orbit. A representation of the concept is shown in **Fig. 1**.

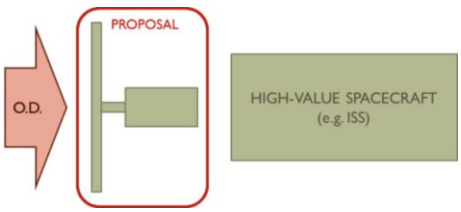

Figure 1. Representation of the initial proposal.

The conceptual design of this "defender" spacecraft was carried out in 3 stages: first, inspired by existing micrometeoroid and orbital debris (MMOD) shield models, a multi-layer shield was designed and tested using Smoothed-Particle Hydrodynamics (SPH) simulations; next, the shield deployment mechanism was designed and analyzed with a vector-based kinematics and dynamics method; and, finally, a general design of the service module, on which both the shield and deployment mechanism would be mounted, was made.

© Springer International Publishing Switzerland 2015, T. Sgobba, I. Rongier (eds.), *Space Safety is No Accident*, DOI 10.1007/978-3-319-15982-9_5

2. MULTI-LAYER SHIELD DESIGN

2.1 Shield configuration

Shield configuration used in analysis consisted of a combination of aluminum mesh and aluminum plate layers (**Fig. 2**). Aluminum mesh was chosen for the first layers because it breaks up projectiles more effectively than a solid plate of the same areal density [8]. After the first few layers of mesh, solid aluminum plate layers were used to slow down and defeat the generated debris cloud.

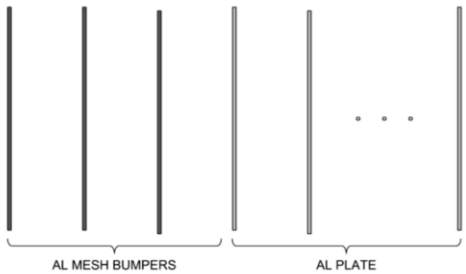

Figure 2. Representation of the Multi-layer shield model.

The initial estimate for the dimensions of the aluminum mesh was made by scaling up the mesh from an existing MMOD shield [8], resulting in a mesh with 2 mm diameter wires in a square pattern with a wire every 5 mm, as seen in **Fig. 3**.

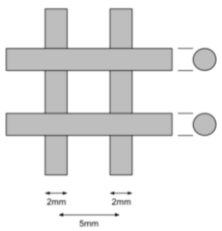

Figure 3. Initial dimensions of the mesh used in the bumper layers.

Numerical simulations were used to determine the minimum required number of aluminum layers.

2.2 Numerical simulations

Traditionally, grid or mesh-based methods, such as the Lagrangian and Eulerian methods, have been used for numerical simulations in many different fields; however, these methods have difficulties dealing with perforation and fragmentation of materials, as is the case in this project [10].

Mesh free methods have become a popular alternative to both Lagrangian and Eulerian grid based techniques. In this project a commercial implementation of mesh-free SPH method [14] was used.

All simulations were executed at a workstation with 2 8-core Xenon E5-2680 CPUs running at 2.7 GHz and 32 Gb of RAM.

Projectiles were modeled as 60x60 mm^2 aluminum plates with a thickness of 5 mm (**Fig. 4**).

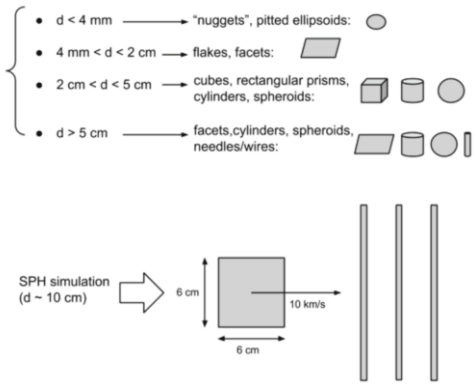

Figure 4. Projectile geometry and orientation used in the SPH simulations.

This geometry was selected because it was simple to implement while still being an adequate representation of the debris population in this size range [12]. The size of the plate was selected taking into consideration that debris sensors and tracking systems are improving; the most recent technologies allow the tracking of debris in LEO as small as 5 cm [13]. Finally, the plate was oriented perpendicular to the shield, as shown in **Fig. 4**, to guarantee its effectiveness in the worst case scenario; and it was given an initial velocity of 10 km/s.

Table 1. Al 7039 material model properties [14], [15].

Name	AL7039
Reference Density [g/cm^3]	2.000

EOS	Shock
Gruneisen coefficient [-]	2.000
Parameter C1 [m/s]	5.328e3
Parameter S1 [-]	1.338
Reference Temp [K]	300
Specific Heat [J/kgK]	874.999

Strength	Johnson Cook
Shear Modulus [kPa]	2.76e7
Yield Stress [kPa]	5.328e3
Hardening constant [kPa]	3.43e5
Hardening exponent [-]	0.410
Strain Rate Constant [-]	0.010
Thermal softening exp [-]	1
Melting Temperature [K]	877
Ref. Strain Rate [/s]	1

Failure	Johnson Cook
Damage Const. D1 [-]	2.76e7
Damage Const. D2 [-]	5.328e3
Damage Const. D3 [-]	3.43e5
Damage Const. D4 [-]	0.410
Damage Const. D5 [-]	0.010
Melting Temperature [K]	877
Ref. Strain Rate [/s]	1

Since all the simulations consisted only of aluminum parts, a single material model was used. The material model used was the high strength AL 7039 aluminum alloy from the available material library, which uses a Shock equation of state (EOS) and Johnson Cook Strength equation [14]. In addition to the provided material properties, a Johnson Cook failure model was

implemented [15]. The material model properties for the AL 7039 alloy used in the simulations are summarized in table 1.

To reduce computational expenses, most of simulations were conducted in 2D. However, for adequate representation of the aluminum mesh in two-dimensional analyses, a few three-dimensional simulations of a single mesh layer under HVI were carried out. They aimed to find an "equivalent-thickness" aluminum plate capable to substitute the mesh in the two-dimensional frame.

The first test that was simulated was the aluminum plate impacting a layer of mesh. This was done in 3D and then a number of 2D simulations with thicknesses for the layer of shielding ranging from 1 to 4 mm were done to compare the results and find the equivalent. Each of the simulations took from 2000 to 3000 computational cycles and around 1 hour to complete.

It was found that the 2 mm aluminum plate produced the closest results to the aluminum mesh, as can be seen in **Fig. 5**, so this was used for the full simulation to represent the mesh layers. In addition, by looking at the debris cloud produced by the first layer of mesh and the portion of the projectile that remains intact, it was estimated that three layers of mesh would be enough to fully break up the projectile and sufficiently spread out the debris cloud.

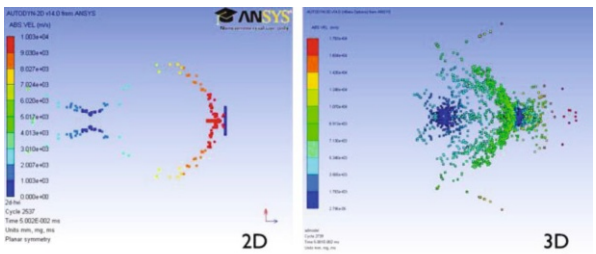

Figure 5. SPH simulation results of a 2mm solid plate in 2D (left) and the 3D aluminum mesh (right).

In the full 2D simulation, overall ten layers were used with the first three layers representing the aluminum mesh. Results of the simulation are shown in **Fig. 6**.

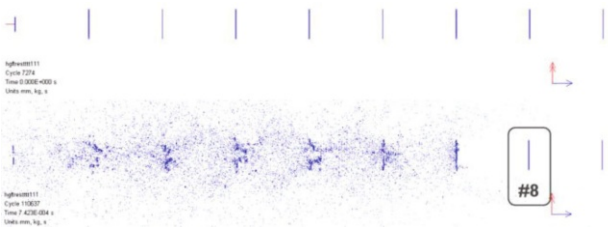

Figure 6. Final SPH simulation results.

It took approx. 110,000 cycles to complete and ran for approximately 80 hours. Once it was completed, the results showed that a total of eight layers were needed to fully defeat the 60x60 mm^2 plate. With 500 mm of standoff between layers this resulted in a total distance of 3.5 m from the first to the last layer. The final shield configuration is shown in **Fig. 7**.

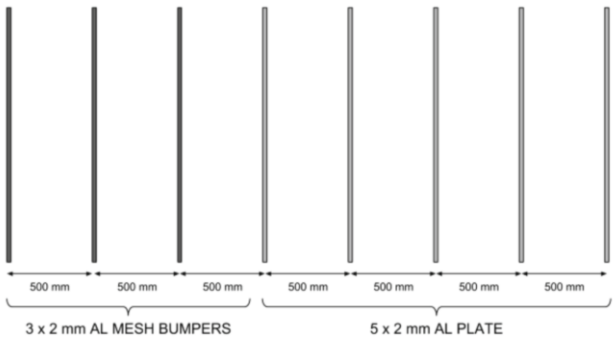

Figure 7. Final shield design dimensions.

It should be noted that, the final shield design was not optimized to minimize its weight, and if the design of this conceptual vehicle for OD protection were to be explored further, a lighter and more effective shield design could be made by considering other possible configurations and materials. For this reason, the design of the deployment mechanism in the next chapter bears in mind the possibility of accommodating different types of shields.

3. SHIELD DEPLOYMENT MECHANISM DESIGN

Of the various possibilities that were considered, the foldable umbrella mechanism was selected in this work for being the most versatile as well as being very compact. Because of its versatility, it fulfilled all of the established requirements: It is a simple mechanism that can easily be adapted to slightly different shapes (e.g. circular, square or rectangular depending on the number and length of branches in the umbrella) and sizes, an example is shown in **Fig. 8**; and the same type of mechanism can be used with flexible fabric-type materials as well as more rigid materials by folding them in on themselves (e.g. paper umbrella).

Having foldable umbrella mechanism as a basis for the final design, some slight modifications were made to adapt it to the specific requirements of this project: An extra link was added to the end of the mechanism shown in **Fig. 8** to extend its reach, the whole mechanism was scaled up to fit a 12 m diameter shield with 8 branches, one every 45º, supporting each layer.

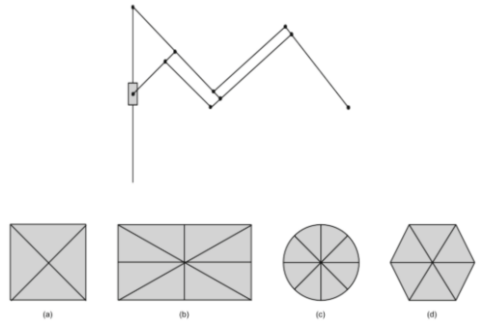

Figure 8. Single branch of a foldable umbrella mechanism next to different possible shapes made with different number and lengths of branches: square (a), rectangle (b), circle (c) and hexagon (d).

Study of the whole mechanism was simplified to the study of a single branch supporting 1/8 of the shield, as seen in **Fig. 9**. At the same time, since in this mechanism every additional layer of shielding followed the same motion as the bottom layer, it was sufficient to analyze only this first layer in the kinematic and dynamic analysis.

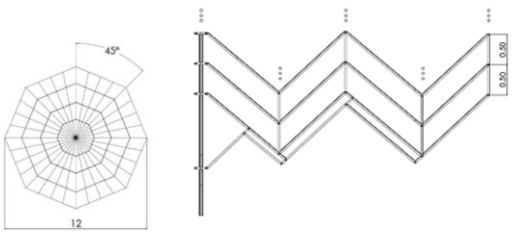

Figure 9. Shield deployment mechanism final design, dimensions in m.

Kinematic and dynamic analysis of the mechanism was made to determine its motion and the resulting forces acting on it as a function of the motion of the slider. This allowed the input motion to be defined in such a way as to minimize the accelerations and, therefore, the inertial forces acting on the mechanism. This analysis was carried out for the simplified mechanism shown in **Fig. 10** using the method described in [16].

Since the mechanism was designed to be opened in orbit, the only forces acting on it were the inertial forces associated with the acceleration of the segments of shielding. With a sinusoidal motion of the slider lasting 10 seconds, the greatest of the four inertial forces acting on each branch of the deployment mechanism was of 25 N. This shows that the implementation of such a mechanism for the shield deployment is feasible. Furthermore, by slowing down the motion of the slider, the resulting accelerations and inertial forces could be decreased even further.

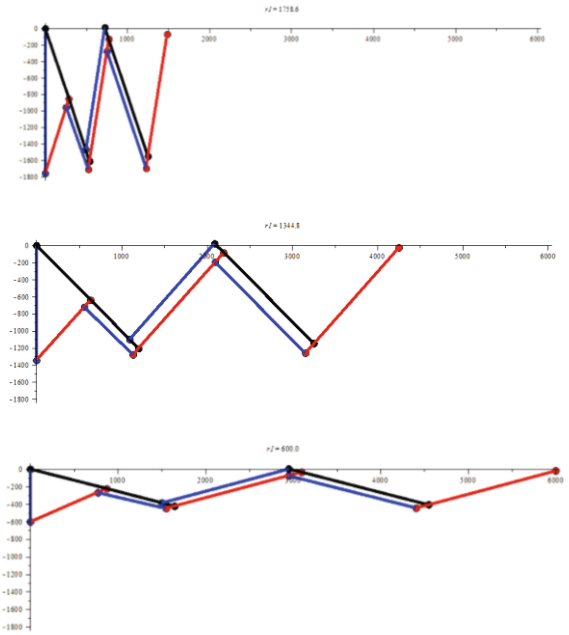

Figure 10. Representation of the final deployment mechanism in three different positions.

4. SERVICE MODULE DESIGN

To conclude the conceptual design, once the shield and the deployment mechanism had been completed, a general design of the rest of the spacecraft that would carry them was made. Since this spacecraft was not intended to carry any payload other than the shield and its deployment mechanism, this stage in the design focused on selecting the components for the service module.

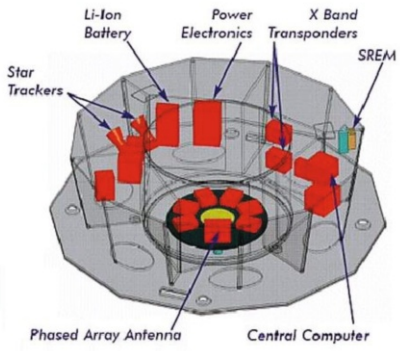

Figure 11. Diagram of the Gaia satellite's service module [17].

To simplify the design, the service module was modelled after that of an existing satellite. The ESA's Gaia

satellite, launched on 19 December 2013, was chosen as the model for the design of the service module. A diagram of Gaia's service module is shown in **Fig. 11** below.

With the Gaia satellite as a reference, the following components were selected for the spacecraft's service module [18], [19]:

a) Micro propulsion system: 12 cold gas thrusters for attitude control on the service module, an additional 12 thrusters on the shield because of its additional mass with respect to the Gaia satellite and an estimate of 100 kg of propellant.

b) Chemical propulsion system: The Gaia satellite required a chemical propulsion system to place it into its Lissajous-type orbit around L2 (Lagrangian Point 2), about 1.5 million km from Earth. In the case at hand no propulsion of this sort was necessary, since the spacecraft is to be placed directly into its desired orbit in LEO. This allowed for a significant reduction in size and mass, by removing the main propulsion system and its propellant.

c) Navigation and control: Three gyroscopes, star trackers, three fine sun sensors for attitude control.

d) Power: Although the shield will generally not be oriented towards the sun, its large area makes it a reasonable location to place solar cells. Alternatively, solar cells could be placed on the side of the spacecraft and shielding, which might provide a higher efficiency. The same six solar cells with a total 12.8 m^2 and 1910 W of capability and 72 Amp-hour battery used in the Gaia satellite should be enough, taking into account the lower power requirement due to the lack of a payload module and the lower efficiency due to non-optimal orientation of the cells. An estimate of the power requirements is shown in table 2.

Since the spacecraft is intended to travel alongside the spacecraft it is protecting (e.g. ISS or other large structures), there is the possibility of linking the two together to share their power. For example, at times when the solar cells of the shield generate excess power, this could be transferred to the spacecraft behind it.

e) Communication system: Three Low Gain Antennas: the medium gain Phased Array Antenna used in the Gaia satellite for science data and telemetry downlink is not required in this case.

f) Thermal tent: CFRP sandwich panels covered with MLI and a thermal radiator. The thermal tent also protects the electronics from radiation and contamination.

Table 2. Estimated power requirements.

Component	Power
RF Communications	326 W
Data Management and AOCS	103 W
Electrical power & solar array	117 W
Propulsion	24 W
TOTAL	**570 W**

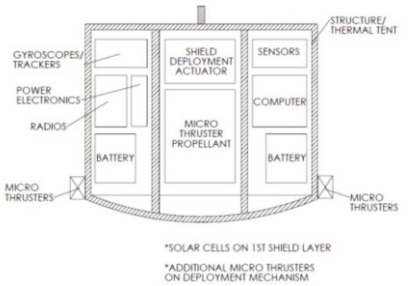

Component	Estimated mass
Service module	800 kg
Micro propulsion propellant	100 kg
TOTAL	**900 KG**

Figure 12. Possible layout for the service module (top) and an estimate of its overall mass (bottom).

With all the basic components selected, a general layout and estimation of the overall weight of the service module were made. Following the model of the Gaia satellite in **Fig. 11**, the service module was housed in a cylindrical structure with a smaller cylinder inside, in which the propellant is stored. The inner cylinder was also made to accommodate the actuator for the shield deployment mechanism. The rest of the components, excepting the thrusters, were located around the inner cylinder. **Fig. 12** exemplifies a cross section of the service module with a diagram showing a possible layout for its components; the module is 2 m in diameter and 1.5 m in height and its estimated mass, 900 kg, is based on the previous component selection.

5. FINAL DESIGN SUMMARY, CONCLUSIONS AND RECOMMENDATIONS

With all three design stages complete, the final design for the spacecraft was put together. This final design is shown in **Fig. 13** and is summarized below.

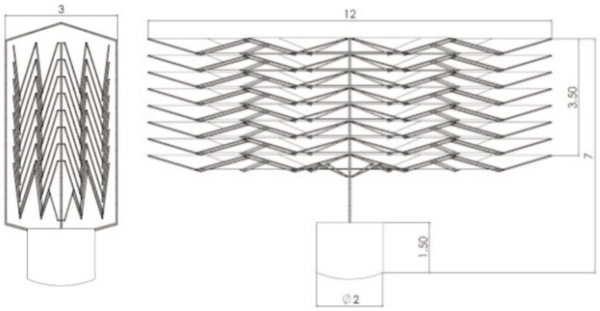

Figure 13. Final design of the "Defender" spacecraft for OD protection, dimensions in m.

a) Orbital debris shield: The orbital debris shield consists of 8 layers of shielding with a 500 mm standoff between each layer; the first three are 2 mm diameter Al 7039 wire mesh in a square pattern with a wire every 5 mm and the next five are 2 mm thick Al 7039 plate. It has an overall areal density of 3.72 g/cm^2 and covers an octagonal area with an outside diameter of 12 m, resulting in a total mass of 4200 kg.

b) Deployment mechanism: The deployment mechanism is based on a foldable umbrella and folds the shield from a 12 m diameter octagonal shape down to a 2.8 m diameter fitted into a 3 m diameter cover. Its final dimensions are shown in **Fig. 14**. The only loads on the mechanism as it opens in orbit are the inertial forces and, therefore, the mechanism can be very lightweight. It's worth mentioning that, although the spacecraft was designed with a 12 m diameter shield, the deployment mechanism can easily be extended to cover a greater area.

c) Service module: The service module, based on that of the Gaia satellite's one, has a 2 m diameter cylindrical structure with a height of 1.5 m and an estimated mass of 900 kg.

Figure 14. Final deployment mechanism dimensions in mm.

Overall, the spacecraft has a 2.8 m diameter and 7 m length when the shield is folded and a 12 m diameter and 7 m length when the shield is deployed. The total mass at launch is estimated at 5100 kg. **Fig. 15** is a 3D render of what the spacecraft could look like in operation.

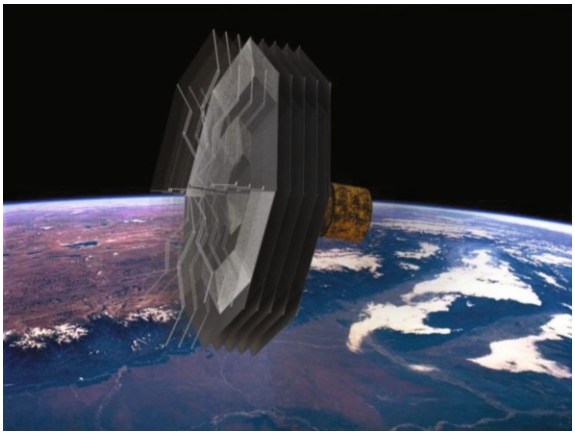

Figure 15. 3D render of the final spacecraft design.

After completing the conceptual design it can be concluded that the use of a "defender" spacecraft of this type for the OD protection of larger structures in orbit is a feasible option that could successfully protect such structures from unforeseeable collisions.

Although a thorough cost analysis would have to be done in each case, the spacecraft's mass and dimensions are within what can be considered reasonable for a satellite in LEO and, therefore, the cost associated with this method of protection should be justifiable for large, high-value spacecraft such as the ISS or missions where the life of astronauts could be at risk. Taking into consideration the growing orbital debris population and the growing probability of impact from objects large enough to cause serious damage to spacecraft but small enough to go undetected, the cost of using a spacecraft of this type for protection would be relatively low compared to the cost of the potential damage from a single collision.

Since this is an initial conceptual design, however, much work remains to be done before this measure could successfully be employed for OD protection. Therefore, recommendations for the further development of this spacecraft are given below.

First, the shield used in the conceptual design was merely the first that was found that fit the requirements; with a more in-depth study, considering alternative materials and layer configurations, the mass of the shield could be greatly reduced. At the same time, the use of fabric based materials, such as Nextel and Kevlar, instead of rigid materials would simplify the deployment mechanism.

As for the deployment mechanism, it was seen that the inertial forces involved were relatively low. Nevertheless, a more in-depth analysis should be made to determine the loads on every bar and joint in the mechanism and optimize their dimensions. Furthermore, the effect on the mechanism of the acceleration at launch and of an impact by a projectile should also be studied.

Finally, since the main focus in this project was the design of the shield and its deployment mechanism, only a general component selection for the service module was made and a more complete design of the service module should be undertaken.

As a final conclusion, even though this is a conceptual design and there is still a lot of work to be done, the project achieved its objective of showing that the use of a spacecraft of this type for orbital debris protection is a feasible option with great potential benefit for the safety of future missions in LEO as well as for the orbital debris environment as a whole.

6. ACKNOWLEDGEMENTS

This work was supported by the University of Manitoba, UPC/Barcelona Tech and partially by a Discovery Grant No. 402115-2012 from the Natural Sciences and Engineering Research Council of Canada.

7. REFERENCES

1. J. Schefter. (1982, July) "The growing peril of space debris," Popular Science, vol. 221 (1), p. 48.
2. ESA. (2013, Apr. 20).
3. A.V. Kudjakov. Concept of the "bodyguard" spacecraft. Personal communication.
4. E.L.Christiansen (1990) "Advanced Meteoroid and Debris Shielding Concepts", AIAA/NASA/DOD Orbital Debris Conference, Technical Issues & Future Directions, Baltimore, MD, pp 1-14.
5. Hypervelocity Impact Shield, by J.L.Crews and B.G.Cour-Palais. (1991). US Patent 5067388
6. Enhanced Whipple Shield, by J.L.Crews, E.L.Christiansen, J.E.Williamsen, J.R.Robinson and A.N.Nolen. (1997). US Patent 5610363 [Online].
7. I. Telitchev and A. Prokhorov. (1997). "Damage parameters analysis of shielded pressure vessels under space debris impact," *Space Debris: Proceedings Of The Second European Conference, ESOC, Darmstadt, Germany, 17-19 March 1997* [Online], vol. 393, pp. 549-552.
8. E. L. Christiansen. (2009). "4.7 Mesh Double-Bumper Shield," in *Handbook for Designing MMOD Protection* [Online]. p. 76. Available: ntrs.nasa.gov/archive/nasa/casi.ntrs.nasa.gov/20090010053_2009007425.pdf.
9. NASA. (23 Oct. 2013). *Hypervelocity Impact Testing* [Online]. Available: ww.nasa.gov/centers/wstf/laboratories/hypervelocity/.
10. G. R. Liu and M. B. Liu. "Introduction," in *Smoothed Particle Hydrodynamics A Mesh Free Method*, Singapore: World Scientific Publishing Co. Pte. Ltd., 2003, pp. 1-32.
11. R. A. Gingold and J. J. Monaghan. "Smoothed particle hydrodynamics - theory and application to non-spherical stars," *Monthly Notices of the Royal Astronomical Society*, vol. 181, pp. 375-389, Nov., 1977.
12. M.D. Hejduk, H.M. Cowardin, and E.G. Stansbery. (2012). "4. Shape information," in *Satellite Material Type and Phase Function Determination in Support of Orbital Debris Size Estimation* [Online]. p.7. Available: ntrs.nasa.gov/archive/nasa/casi.ntrs.nasa.gov/20120015337_2012015216.pdf.
13. NASA. (2013, Sept. 27). *Space Debris and Human Spacecraft* [Online]. Available: www.nasa.gov/mission_pages/station/news/orbital_debris.html#.Uxor5_mwIRo.
14. *ANSYS Autodyn v. 14.0*. ANSYS, Inc., 2011.
15. B.M. Corbett. (2006). "Numerical simulations of target hole diameters for hypervelocity impacts into elevated and room temperature bumpers," *International Journal of Impact Engineering*, vol. 33 (1-12), pp. 431-440.
16. O. Vinogradov. *Fundamentals of Kinematics and Dynamics of Machines and Mechanisms* [Online]. New York: CRC Press, 2000.
17. ESA. "ESM-400.gif" [Online]. Available: http://sci.esa.int/science-e-media/img/c2/ESM-400.gif.
18. ESA. (2013, March 17). *Gaia* [Online]. Available: http://sci.esa.int/gaia/40128-overview/.
19. P. Blau. (2013). "Gaia spacecraft overview" *Spaceflight101*. [Online]. Available: www.spaceflight101.com/gaia-spacecraft-overview.html.